Journal of the Optical Society of Korea
Vol. 19, No. 6, December 2015, pp. 679-686

ISSN: 1226-4776(Print) / ISSN: 2093-6885(Online)
DOI: http://dx.doi.org/10.3807/JOSK.2015.19.6.679

Design of a Tele-centric Wide Field Lens with High Relative Illumination and Low Distortion Using Third-order Aberration Analysis

Kae-Hong Kim, Yeong-Sik Kim, and Sung-Chan Park*

Department of Physics, Dankook University, Cheonan 31116, Korea

(Received October 2, 2015 : accepted November 27, 2015)

This paper presents a design method for improving the low relative illumination and large distortion due to widening the field of a system. A tele-centric optical system in image space was suggested to increase the relative illumination. Through the analyses of the third-order aberrations affected by introducing aspherical surfaces, we have proposed a method to determine analytically what surface should be aspheric to correct each aberration effectively. By utilizing this method to design a wide field lens, a tele-centric wide field lens with f-number of F/2.0 was obtained. Even though the field angle is 120 degrees, it has a very low distortion less than -2% and high relative illumination more than 73.7%. In conclusion, this analytic method for selecting aspherical surfaces is expected to serve as a useful way to find design solutions.

Keywords : Wide field, Distortion, Third order aberrations, Telecentric system
OCIS codes : (220.3620) Lens system design; (220.0220) Optical design and fabrication; (080.0080) Geometric optics

I. INTRODUCTION

In modern optical instruments such as CCTV and black box cameras, a wide field system is widely used. Such a system is required to cover an extremely wide field, normally more than 120 degrees, without additional instruments. Because of its inherent wide angle, however, the large incidence angles of rays into an image plane significantly reduces the illumination around the margin field and induces large aberrations, especially great distortion being proportional to the cube of field size [1]. Many wide field lenses subtending the field angle of 120 degrees have been reported, but their distortions are from -40% to -50% [2-4]. These distortions are so large that the images are significantly distorted, to a level that needs soft-ware to correct distorted images.

To overcome these problems, in this paper we propose a design method for improving the low relative illumination and large distortion due to widening the field of a system. A tele-centric optical system in image space is suggested to reduce the incidence angles of rays into an image, which results in increasing the relative illumination [5-8].

All the third-order aberrations can be corrected by introducing aspherical surfaces. Through the analyses of the third-order aberrations affected by aspherical parameters [9-11], this study proposes a method to determine analytically the aspheric surface that is most effective to correct each aberration. From the aberration analyses, aspherization of rear surface of the 1st lens is confirmed to be most appropriate for distortion correction.

By utilizing this design method, a tele-centric wide field lens with field angle of 120 degrees has been obtained. In addition, it has a very small distortion less than -2% at the margin field.

II. DESIGN OF A TELE-CENTRIC SYSTEM

In this study, to overcome low illumination due to wide field, a tele-centric optical system in image space is suggested to improve the relative illumination. The starting wide field lens is selected from the patented lens composed of two groups, as shown in Fig. 1 [2]. This lens can realize the wide field, but has great distortion of -48.53% at the margin field. The goal of our study is to design an optical

*Corresponding author: scpark@dankook.ac.kr

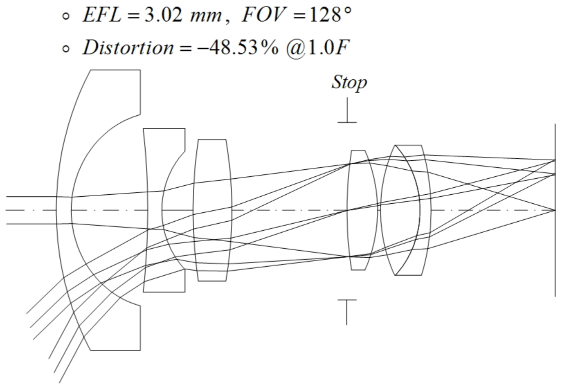

FIG. 1. Patented lens for a wide field camera (US Patent 8,917,460 B2).

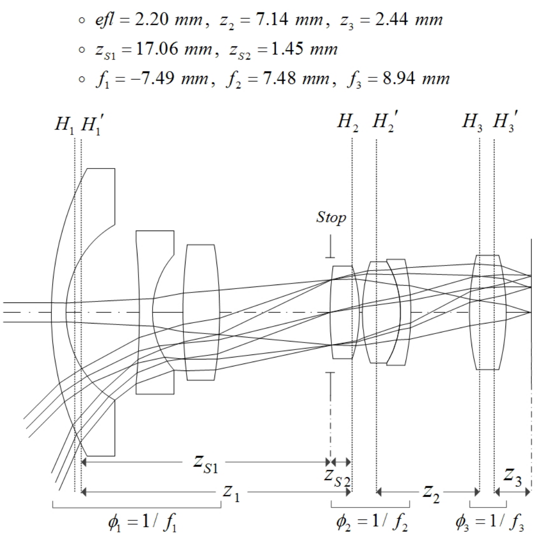

FIG. 2. Layout of a tele-centric optical system obtained by locating a positive element (ϕ_3).

system having small distortion less than ±2% and higher relative illumination at all fields, by using the proposed design concepts.

In Fig. 1, the configuration of a negative first group and positive second group gives a retro-focus system so that it is suitable for a wide field lens. Our tele-centric system can be realized by adding a lens element before the image plane, as shown in Fig. 2.

By denoting the distances between adjacent principal planes as z_i ($i = 1, 2, 3$), the focal length ($efl = 1/\phi_t$), imagery condition of an axial ray (z_3), and tele-centric condition are given [4, 5], as follows:

$$[\phi_1, -(z_{s1} + z_{s2}), \phi_2, -z_2, \phi_3] = \phi_t \,, \tag{1}$$

$$[\phi_1, -(z_{s1} + z_{s2}), \phi_2, -z_2, \phi_3, -z_3] = 0 \,, \tag{2}$$

$$[-z_{s2}, \phi_2, -z_2, \phi_3] = 0 \,. \tag{3}$$

Solving Eqs. (1)~(3) simultaneously results in an expression for the unknown parameters of

$$\phi_3 = \frac{\phi_t(-1+\phi_2 z_{s2})}{-1+\phi_1 z_{s2}} \tag{4}$$

$$z_2 = \frac{-1+\phi_1 z_{s1}+\phi_t z_{s2}}{\emptyset_t(-1+\phi_2 z_{s2})} \,, \tag{5}$$

$$z_3 = \frac{(-1+\phi_1 z_{s1})(\phi_t-\phi_1-\phi_2+\phi_1\phi_2 z_{s1}+\phi_1\phi_2 z_{s2})}{{\phi_t}^2(-1+\phi_2 z_{s2})} \,. \tag{6}$$

Figure 2 illustrates the tele-centric system found by locating the element designed from Eqs. (4)~(6).

III. PROJECTION METHOD IN A WIDE FIELD LENS

The full field angle of the system is aimed to 120°, therefore the gnomonic projection method is generally used to define the image size [6, 12-13]. The paraxial image height ($\bar{y}_i$) and distortion (%) are respectively given by

$$\bar{y}_i = f \; \tan\theta \,, \tag{7}$$

$$Distortion(\%) = \frac{\bar{y}_r - \bar{y}_i}{\bar{y}_i} \times 100 \,. \tag{8}$$

If the real image height ($\bar{y}_r$) and full field angle (2θ) subtending an image sensor are given, the focal length can be determined to make a system have targeted distortion. In other words, if the distortion is allowed to ±2%, the paraxial image height is calculated from Eq. (8) at a given sensor size, and inserting it into Eq. (7) gives the range of focal lengths. Table 1 lists the ranges of focal lengths for several image sensors, which can correct distortion within ±2% at field angle of 120 degrees.

TABLE 1. Ranges of EFLs for several image sensors to correct distortion within ±2% at field angle of 120 degree

Sensors	Image heights ($\bar{y}_r$)	Ranges of EFLs
1/3 inch	3.0 mm	1.698 mm ~ 1.767 mm
1/4 inch	2.2 mm	1.245 mm ~ 1.296 mm
1/5 inch	1.8 mm	1.019 mm ~ 1.060 mm

IV. ANALYSES OF THE THIRD-ORDER ABERRATIONS OF A LENS SYSTEM

The third-order aberration coefficients for spherical aberration (S_I), coma (S_{II}), astigmatism (S_{III}), Petzval blur (S_{IV}), and distortion (S_V) of a system are expressed, as [9-11]

$$S_I = \sum_{j=1}^{l} (ni)_j{}^2 y_j \left(\frac{u_j}{n_j} - \frac{u_{j-1}}{n_{j-1}}\right), \quad (9)$$

$$S_{II} = \sum_{j=1}^{l} (ni)_j (n\bar{i})_j y_j \left(\frac{u_j}{n_j} - \frac{u_{j-1}}{n_{j-1}}\right), \quad (10)$$

$$S_{III} = \sum_{j=1}^{l} (n\bar{i})_j{}^2 y_j \left(\frac{u_j}{n_j} - \frac{u_{j-1}}{n_{j-1}}\right), \quad (11)$$

$$S_{IV} = H^2 \sum_{j=1}^{l} P_j = H^2 \sum_{j=1}^{l} c_j \left(\frac{1}{n_j} - \frac{1}{n_{j-1}}\right), \quad (12)$$

$$S_V = \sum_{j=1}^{l} \frac{(n\bar{i})_j}{(ni)_j} \left\{H^2 P_j + (n\bar{i})_j{}^2 y_j \left(\frac{u_j}{n_j} - \frac{u_{j-1}}{n_{j-1}}\right)\right\}, \quad (13)$$

where

$$(ni)_j = n_j(c_j y_j - u_j),$$

$$(n\bar{i})_j = n_j(c_j \bar{y}_j - \bar{u}_j), \quad (14)$$

$$H = n_j \bar{u}_j y_j - n_j u_j \bar{y}_j .$$

In these equations, u_j and y_j ($j = 1, 2, \cdots, l$) are the convert-gence angle and height of the ray from the axial object point, also $\bar{u}_j$ and $\bar{y}_j$ ($j = 1, 2, \cdots, l$) are the convergence angle and height of the chief ray from the off-axial object point. P_j ($j = 1, 2, \cdots, l$) is the Petzval curvature of the jth surface, also c_j and cn_j are the curvature and refractive index of the jth surface.

The conic constant (k) and fourth-order coefficient (A) of an aspheric surface have an effect on the third-order aberrations, meanwhile the higher-order coefficients (B, C, D, ⋯) are useful in correcting the higher-order aberrations. The equation for the aspheric surface is given as

$$z = \frac{cy^2}{1+[1-(1+k)c^2y^2]^{1/2}} + \mathrm{A}y^4 + \mathrm{B}y^6 + \mathrm{C}y^8 + \mathrm{D}y^{10} + \cdots . \quad (14)$$

Introducing the conic constant (k_j) and fourth-order coefficient (A_j) into the jth surface generates the additional third-order aberrations, as follows [9-11]:

Spherical aberration: $\Delta S_{I\,j} = PA_j(y_j{}^4)$, (15)

Coma: $\Delta S_{II\,j} = PA_j(\bar{y}_j y_j{}^3)$, (16)

Astigmatism: $\Delta S_{III\,j} = PA_j(\bar{y}_j{}^2 y_j{}^2)$, (17)

Distortion: $\Delta S_{V\,j} = PA_j(\bar{y}_j{}^3 y_j)$, (18)

where

$$PA_j = (k_j c_j{}^3 + 8A_j)(n_{j-1} - n_j). \quad (19)$$

Therefore the conditions that all the third-order aberrations except Petzval blur are corrected, by combining Eqs. (9)~(13) with Eqs. (15)~(18), are expressed as follows:

$$S_I + \Delta S_{I\,j} = 0, \quad (20)$$

$$S_{II} + \Delta S_{II\,j} = 0, \quad (21)$$

$$S_{III} + \Delta S_{III\,j} = 0, \quad (22)$$

$$S_V + \Delta S_{V\,j} = 0. \quad (23)$$

V. DESIGN FOR AN INITIAL WIDE FIELD LENS USING THE THIRD-ORDER ABERRATION ANALYSES

In this research, unlike general methods correcting the aberrations using aspheric surfaces, we suggest approaches to analytically determine what surface is most effective to correct each third-order aberration. Before determining these corrections, Petzval curvature should be firstly removed from the spherical lens, not the aspheric.

5.1. Petzval Field Curvature Correction

In Section Ⅱ, adding a positive element in front of an image gave a tele-centric system, but in parallel it made the system have a much more negative Petzval sum. Since the selection of optical glasses is limited, it is better to change the curvature than the refractive index so that the Petzval sum can be easily corrected.

Because the first group is located before the stop, even if its parameters are changed, the tele-centric system is still effective. To have zero Petzval sum, the radius of curvature of the jth surface is required to have the value given by Eq. (24).

$$r_j = \frac{1}{-\sum_{i\neq j}^{13} P_i}\left(\frac{1}{n_j} - \frac{1}{n_{j-1}}\right), \tag{24}$$

where j = 1, 2, ⋯, 6.

In Eq. (24), the denominator denotes the Petzval sum except the Petzval curvature of the jth surface. Consequently, the radius of curvature of each surface can be calculated to have zero Petzval sum, and Table 2 lists the calculated radius of curvature of each surface to make the Petzval sum be zero.

To have zero Petzval sum in Table 2, changing the radius of the 4th surface (r_4) is most effective, because its rate of change is the smallest. But if r_4 is chosen, it should be reduced to 2.516 mm, which is too small to have a necessary aperture size. Changing the radius of the 2nd surface (r_2) gives a similar result. So, two radii of r_2 and r_4 are selected to correct the Petzval sum. The additional Petzval curvature, being induced from adding a lens element, can be canceled out by changing two radii of curvature of minus lenses. After allocating the additional Petzval curvature to two surfaces so that they are proportional to the rates of change of Table 2, two radii of r_2 and r_4 are changed to correct each additional Petzval curvature. Table 3 shows two radii of curvature correcting the Petzval sum. Also this system is still satisfying the tele-centric condition. During this design process, the focal length has been changed to 1.294 mm, which can realize the system having distortion of ±2%, if a 1/4-inch image sensor is selected from Table 1.

5.2. Spherical Aberration Correction Using Conic Constant

Among the third-order aberrations, we firstly correct spherical aberration using an aspherical surface. By introducing an aspheric to the jth surface, the condition that spherical aberration is corrected is expressed in terms of a conic constant (k_j) and fourth-order coefficient (A_j), as [9-11]

$$\left(k_j c_j^3 + 8A_j\right)\left(n_{j-1} - n_j\right) = -\frac{1}{(y_j^4)} S_I\,. \tag{25}$$

For $A_j = 0$, Equation (25) is reduced to

$$k_j = -\frac{1}{c_j^3(n_{j-1}-n_j)(y_j^4)} S_I\,. \tag{26}$$

Introducing an aspheric to the 7th surface at stop has advantage in that any aberration is not changed, except for spherical aberration. For spherical aberration to be corrected, from Eq, (26), the conic constant of the 7th surface should be k_7 = -14.964. This lens system is still satisfying the zero Petzval sum and tele-centric condition.

5.3. Correction of Spherical Aberration and Distortion

By aspherization of the 7th and other surfaces, we can simultaneously correct spherical aberration and distortion that is the most troubling aberration in a wide field system. From Eqs. (15), (18), (20), and (23), the following equations must be satisfied for these aberrations to be corrected:

$$S_I + PA_7(y_7^4) + PA_j(y_j^4) = 0\,, \tag{27}$$

$$S_V + PA_7(\bar{y}_7^3 y_7) + PA_j(\bar{y}_j^3 y_j) = 0\,. \tag{28}$$

Assuming that two fourth-order coefficients(A_7, A_j) are zero and solving the above two equations, the solutions for A_7 and k_j are given by

$$k_7 = -\frac{1}{c_7^3(n_6-n_7)} \times \frac{y_j^3 S_V - \bar{y}_j^3 S_I}{\bar{y}_j^3 y_7^4 - \bar{y}_7^3 y_j^3 y_7}, \tag{29}$$

$$k_j = -\frac{1}{c_j^3(n_{j-1}-n_j)} \times \frac{y_7^3 S_V - \bar{y}_7^3 S_I}{\bar{y}_7^3 y_j^4 - \bar{y}_j^3 y_7^3 y_j}. \tag{30}$$

Table 4 shows the conic constants of k_7 and k_j that correct spherical aberration and distortion simultaneously. The new conic constant of k_7, being used to correct spherical aberration, should be selected to be not far away from the initial value of k_7 = -14.964. Because the conic constant (k_2) of the 2nd surface is smallest, aspherization for the second surface is most desirable to have distortion be removed. By selecting k_2 = -1.057 and k_7 = -15.163, we can obtain the optical system corrected for distortion and spherical aberration.

5.4. Correction of Spherical Aberration, Distortion, and Astigmatism

The 2nd and 7th surfaces are aspherized to correct distortion

TABLE 2. Calculated radius of curvature of each surface to correct the Petzval sum

Surface	Initial radius	Calculated radius	Rate of change
1	17.09 mm	-8.428 mm	-149.31%
2	6.00 mm	2.908 mm	-51.53%
3	-42.73 mm	-4.528 mm	-89.40%
4	5.00 mm	2.516 mm	-49.68%
5	29.55 mm	-7.640 mm	-125.85%
6	-23.30 mm	8.240 mm	-135.23%

TABLE 3. Radii of curvature to correct the Petzval sum

r_2	3.893 mm
r_4	3.368 mm
Petzval sum: $\sum_{i=1}^{13} P_i = 0$	

TABLE 4. Conic constants to correct spherical aberration and distortion

Surface	k_7	k_j
j=1	-15.098	54.435
j=2	**-15.163**	**-1.057**
j=3	-24.774	-9122.132
j=4	-31.612	-6.117
j=5	-105.915	2673.235
j=6	-241.972	1577.838
j=8	203896.053	-12963.138
j=9	135687.588	-11289.260
j=10	11005.059	593.195
j=11	7265.314	-2228.071
j=12	168.416	-603.477
j=13	24.171	-565.557

and spherical aberration. By introducing an aspheric into another surface, the conditions for correction of astigmatism and the above two aberrations are given by

$$S_{I} + PA_2(y_2{}^4) + PA_7(y_7{}^4) + PA_j(y_j{}^4) = 0\,, \tag{31}$$

$$S_{III} + PA_2(\bar{y}_2{}^2 y_2{}^2) + PA_7(\bar{y}_7{}^2 y_7{}^2) + PA_j(\bar{y}_j{}^2 y_j{}^2) = 0\,, \tag{32}$$

$$S_{V} + PA_2(\bar{y}_2{}^3 y_2) + PA_7(\bar{y}_7{}^3 y_7) + PA_j(\bar{y}_j{}^3 y_j) = 0\,. \tag{33}$$

Assuming that three fourth-order coefficients (A_2, A_7, A_j) are zero and solving three simultaneous equations Eqs. (31)~(33), the parameters of k_2, k_7, and k_j can be calculated for all surfaces that may be aspherized. Table 5 illustrates the conic constants of k_2, k_7, and k_j that correct distortion, spherical aberration, and astigmatism simultaneously.

The conic constant k_2, being used for distortion correction in the previous section, has changed astigmatism from positive to negative value. Because astigmatism is over-corrected, it is desirable to select the surface that gives the k_2 less than -1.057 of Table 4 with small k_7 and k_j for corrections of spherical aberration and astigmatism. From Table 5, selection of k_2 = -1.017, k_7 = -8.135, k_{12} = -23.103 gives a good solution which removes distortion, spherical aberration, and astigmatism.

5.5. Correction of All Third-Order Aberrations

Among the third-order aberrations, the Petzval sum was already corrected using two negative surfaces of the front group, and three aberrations other than coma were also removed by asphterization of three surfaces. By introducing another aspherical surface, the conditions correcting all the third-order aberrations are given by

TABLE 5. Conic constants to correct distortion, spherical aberration, and astigmatism simultaneously

Surface	k_2	k_7	k_j
j=1	2.458	-14.946	181.000
j=3	-1.220	-13.682	1406.068
j=4	-1.186	-13.159	0.745
j=5	-1.122	-9.599	-163.891
j=6	-1.103	-5.299	-68.619
j=8	-1.053	807.696	-52.311
j=9	-1.052	611.168	-52.105
j=10	-1.046	100.588	6.231
j=11	-1.044	72.308	-26.769
j=12	**-1.017**	**-8.135**	**-23.103**
j=13	-0.993	-12.792	-34.090

TABLE 6. Conic constants to correct distortion, spherical aberration, astigmatism, and coma simultaneously

Surface	k_2	k_7	k_{12}	k_j
j=1	-2.456	-5.313	-32.674	-74.983
j=3	-0.950	-6.316	-30.682	-461.231
j=4	-0.964	-6.570	-30.302	-0.232
j=5	-0.990	-7.766	-28.927	41.315
j=6	-0.998	-8.753	-28.135	14.944
j=8	**-1.018**	**31.229**	**-21.988**	**-2.524**
j=9	-1.019	26.630	-21.806	-2.925
j=10	-1.021	8.699	-19.526	0.965
j=11	-1.022	6.931	-18.776	-5.014
j=13	-1.043	-2.908	-49.032	38.260

$$S_{I} + PA_2(y_2{}^4) + PA_7(y_7{}^4) + PA_{12}(y_{12}{}^4) + PA_j(y_j{}^4) = 0\,, \tag{34}$$

$$S_{II} + PA_2(\bar{y}_2 y_2{}^3) + PA_7(\bar{y}_7 y_7{}^3) + PA_{12}(\bar{y}_{12} y_{12}{}^3) + PA_j(\bar{y}_j y_j{}^3) = 0\,, \tag{35}$$

$$S_{III} + PA_2(\bar{y}_2{}^2 y_2{}^2) + PA_7(\bar{y}_7{}^2 y_7{}^2) + PA_{12}(\bar{y}_{12}{}^2 y_{12}{}^2) + PA_j(\bar{y}_j{}^2 y_j{}^2) = 0\,, \tag{36}$$

$$S_{V} + PA_2(\bar{y}_2{}^3 y_2) + PA_7(\bar{y}_7{}^3 y_7) + PA_7(\bar{y}_7{}^3 y_7) + PA_j(\bar{y}_j{}^3 y_j) = 0\,. \tag{37}$$

Through the same design process of Section 5.4, solving four simultaneous equations of Eqs. (34)~(37) provides the values of k_2, k_7, k_{12}, and k_j for all surfaces that may be aspherized. Table 6 illustrates the conic constants of k_2, k_7,

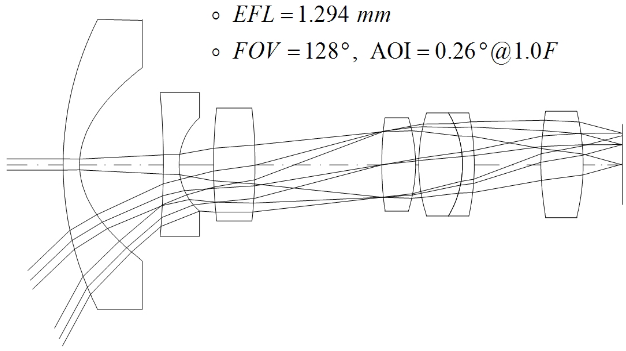

FIG. 3. A tele-centric optical system of which all the third-order aberrations are corrected.

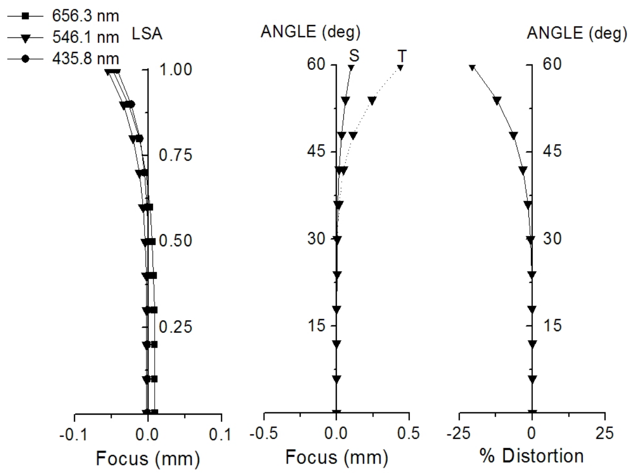

(a) (b) (c)

FIG. 4. Ray aberrations of a tele-centric optical system of which all the third-order aberrations are corrected: (a) Longitudinal spherical aberration, (b) astigmatic field curves, and (c) distortion.

k_{12}, and k_j that correct the third-order aberrations.

In the aberrations correction of Section 5.4, the best three surfaces are independently selected to correct three aberrations so that three aspheric lenses are required. In this study, we hope to use just three aspherical lenses without an additional aspherical lens. Therefore, the 1st, 8th, and 13th surfaces can be aspherized to correct coma. Since the 8th surface is near to a stop, the height of a chief ray is low, and that of an axial marginal ray is high. Therefore, aspherization of the 8th surface is very useful in removing coma aberration. From Table 6, the design parameters of $k_2 = -1.018$, $k_7 = 31.229$, $k_{12} = -21.988$, and $k_8 = -2.524$ give a good solution for correction of distortion, spherical aberration, astigmatism, and coma simultaneously.

Figure 3 shows a tele-centric optical system of which all the third-order aberrations are corrected, and Fig. 4 illustrates the ray aberrations of this system.

VI. COMPLETE WIDE FIELD LENS DESIGN

A tele-centric system of Fig. 3 has been designed to have the focal length of 1.294 mm, which is proper to realize the system having distortion of ±2%, if a 1/4-inch image sensor is used, as shown in Table 1. In the initial design, however, we corrected the third-order aberrations useful in reduced aperture and field so that practicable aperture and image size were small. If current specifications for a wide angle camera are to be met, the aperture and field size should be increased. The aperture is extended to F/2.0. The full field size is increased to 4.4 mm for a 1/4-inch CCD, which corresponds to 120 degree at focal length of 1.294 mm. In an extended aperture and field system, however, there are higher-order aberrations that are not corrected in the previous design, as shown in Fig. 4.

In order to improve the overall performance of the lens system with an extended aperture and field, we balance the aberrations of the starting lens given in Fig. 3 by using the higher-order aspheric coefficients not used in correction of the third-order aberrations.

Finally, a wide field lens having good performance is obtained. The layout of the system is shown in Fig. 5. Table 7 lists the specifications of this lens. Compared to

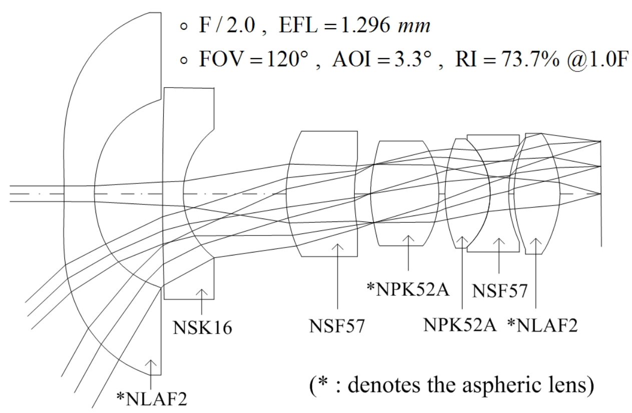

FIG. 5. Layout of an aberration-balanced wide field lens.

TABLE 7. Specifications for a wide field camera lens

Items	Target specification	Final design specification
Sensor	1/4 inch (1.75 μm × 1.75 μm)	
Focal length(mm)	1.245~1.296	1.296
F/no	F/2.0	F/2.0
Field of view	120°	120°
Chief ray angle	±5°	+3.3°
Exit pupil distance	infinity	9.5×10^6 mm
Distortion	±2%	-1.99%
Relative illumination	50% at 1.0F	73.7%
Modulation transfer function (%) at 200 lp/mm	50% at 0.0F	72.6%
	30% at 1.0F	34.8%

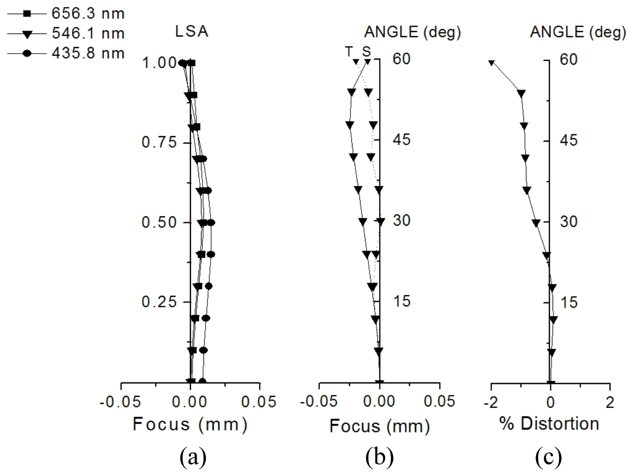

FIG. 6. Ray aberrations of an aberration-balanced wide field lens: (a) Longitudinal spherical aberration, (b) astigmatic field curves, and (c) distortion.

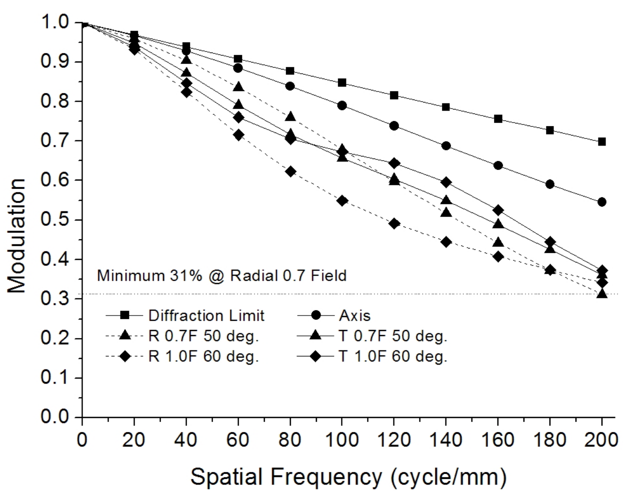

FIG. 7. MTF characteristics of an aberration-balanced wide field lens.

Fig. 4, all residual aberrations are significantly reduced, as shown in Fig. 6. Especially distortion is dramatically reduced to -2%, from 48.53% of the patented lens. Even though this system covers an extremely wide field angle of 120 degrees, distortion is so small that the distorted image is nearly not seen.

Figure 7 shows the modulation transfer function (MTF) characteristics of the system. The MTF at 200 *lp/mm* is more than 31% over all fields. Also, the ratio of relative illuminations is more than 73.7% at all fields. The chief ray's angle of incidence (AOI) into the image plane is just +3.3° at margin field. It is so small that this lens is near to a tele-centric system, as targeted in the starting design.

Even though it is extremely wide angle, the total track of the lens is just 23.56 mm, and large aperture with F/2.0 is realized. Consequently, this system has enough performance to fulfill the requirements of a modern wide field camera.

VII. CONCLUSION

By use of the third-order aberration analyses and tele-centric design, in this paper large distortion and low relative illumination due to widening the field have been solved. To correct all the third-order aberrations without changing configuration, aspheric lenses are most effective so that they are used to correct aberrations.

In a design using general software like Code-V, the designer usually determines the surfaces to be aspherized from empirical judgments. Through the analyses of the third-order aberrations affected by aspherical parameters, however, this study proposed the method to determine analytically what surface should be aspheric to correct each aberration effectively. By utilizing this method to design a wide field lens, an initial tele-centric system was obtained, of which all the third-order aberrations were removed. To improve the performance of the starting lens in the extended aperture and field, three aspheric lenses are used to balance the residual aberrations.

A wide field lens with a total track of 23.56 mm, whose aperture was F/2.0, was obtained. In addition, even though this lens subtends the field angle of 120 degree, it has a very low distortion less than -2%. The optical system developed in this work performs reasonably as a compact camera system with wide field angle. In conclusion, this analytic method for selecting aspherical surfaces is expected to serve as a useful way to find design solutions.

REFERENCES

1. C. S. Rim, "The study of fisheye lens for the causes of rapid illumination drop and the ways to correct on an image sensor due to an ultra wide angle of view," Korean J. Opt. Photon. (Hankook Kwanghak Hoeji) **23**, 179-188 (2012).
2. M. W. Kang, "Fixed focus lens system," U. S. Patent 8917460 (2014).
3. K. Ono, "Wide-angle lens, and imaging device," W. O. Patent 2014087602 (2014).
4. I. Abe, H. Yoshida, and N. Moniwa, "Wide-angle lens and imaging apparatus using the same," U. S. Patent 0169912 (2011).
5. M. P. Rimmer, "Relative illumination calculations," Proc. SPIE **0655**, 99-104 (1986).
6. J. W. Kim, J. M. Rye, and Y. J. Kim, "Tolerance analysis and compensation method using Zernike polynomial coefficients of omni-directional and fisheye varifocal lens," J. Opt. Soc. Korea **18**, 720-731 (2014).
7. M. Watanabe and S. K. Nayar, "Telecentric optics for computational vision," in *Lecture Notes in Computer Science, ECCV '96*, B. Buxton and R. Cipolla eds. (Cambridge, UK, 1996), vol. 1065, pp. 439-451.
8. M. Watanabe and S. K. Nayar, "Telecentric optics for focus analysis," IEEE Transactions on Pattern Analysis and

Machine Intelligence **19**, 1360-1365 (1997).
9. R. E. Hopkins and R. Hanau, *Military Standardization on Hand Book: Optical Design* (MIL-HDBK-141, Washington D.C., USA, 1962), Section 8-10.
10. W. J. Smith, *Modern Optical Engineering*, 3rd ed. (McGraw-Hill Inc., New York, USA, 2001), Chapter 2, 3, 10.
11. W. T. Welford, *Aberrations of the Optics Systems* (Adam Hilger Ltd., Bristol, 1986), pp. 130-158.
12. B. Hönlinger and H. H. Nasse, "Distortion," (Carl Zeiss AG, Germany, October, 2009).
13. G. I. Kweon, S. U. Hwang-bo, G. H. Kim, S. C. Yang, and Y. H. Lee, "Wide-angle cata-dioptric lens with a rectilinear projection scheme," Proc. SPIE **5962**, 624125 (2005).